

Ion Dynamics under Pressure in an Ionic Liquid

A. Rivera-Calzada,^{*,†} K. Kaminski,[‡] C. Leon,[†] and M. Paluch[‡]

GFMC, Dpto. Física Aplicada 3, Universidad Complutense de Madrid, Spain, and Institute of Physics, Silesian University, Katowice, Poland

Received: October 30, 2007; In Final Form: December 4, 2007

We investigate ion dynamics under pressure in the ionic liquid 1-butyl-1-methylpyrrolidinium bis[oxalate]borate (BMP-BOB) by conductivity relaxation measurements in the temperature range 123–300 K and varying pressures from 0.1 MPa up to 0.5 GPa. We report on the influence of pressure on the relaxation times and on the spectral shape of the conductivity relaxation process. We also analyze the pressure dependence of the glass transition temperature and find that the dynamic response under pressure in this ionic liquid shows remarkable similarities to nonionic glass formers. The main relaxation process shows temperature–pressure superposition while a secondary relaxation process, very weakly depending on pressure, is observed. The spectral shape of the main relaxation broadens with increasing pressure or decreasing temperature, but is found to be the same when the relaxation time is the same, independently of the particular pressure and temperature values.

Introduction

Ionic liquids (IL) are receiving increasing research effort during past years.^{1–3} Because of their ionic character, they show properties different from those of the molecular liquids, which make them very attractive for technological applications like electro-depositions, battery electrolytes, and as solvents for a wide range of chemical reactions. Ionic liquids consist exclusively of anions and cations, like conventional salts such as NaCl, and in case a special bulky asymmetric organic molecule is chosen as a cation, they can be liquid down to unusually low temperatures, even well below room temperature. Of most importance is the nonmeasurable vapor pressure of IL, which promoted these chemicals during the past decade as perfect candidates for environmentally friendly or “green” chemistry, substituting the toxic organic solvents used up to now in industrial processes.^{1–3}

Ionic liquids typically exhibit different bonding interactions, from H-bonds to the usual van der Waals interactions, but, unlike in other liquids, they are characterized by the presence of Coulomb interactions among the constituent ions. Thus, as many ionic liquids are easily supercooled, they may introduce a rich phenomenology in the dynamics of the supercooled liquid close to the glass transition. The glass transition is characterized by a dramatic slowing of the characteristic times of the structural relaxation, and because dielectric (conductivity) spectroscopy allows one to follow this process in the widest time/frequency window, it is a technique vastly used to probe the dynamics of liquids and polymers in the supercooled and glassy states.^{4,5} Most of these studies deal with the temperature dependence of the materials at atmospheric pressure, but recently an increasing number of works have outlined that important information can be accessed by using pressure as a variable.^{5–7} Specifically, pressure provokes only density changes while temperature varies both activation energy and density. Accordingly, the pressure

dependence of the glass transition temperature T_g , or the pressure–temperature superposition, are experimental facts that should be accounted for in any theory or model of the glass transition.^{7,8}

Although relaxation dynamics in ionic liquids have been investigated in the past,^{9–12} the influence of pressure on their dynamics has not been reported yet. A detailed work on viscosity and dc conductivity measurements has shown, for example, an unexpectedly large range of fragilities for ionic liquids.⁹ These materials develop a long-range conductivity like standard ionic conductors,^{13–16} as reported in the case of $\text{Ca}_{0.4}\text{K}_{0.6}(\text{NO}_3)_{1.4}$ (CKN),¹⁷ but their dynamic response keeps the ingredients of molecular glass formers. Also, the characteristic secondary relaxations, regarded as a fundamental characteristic of the glassy state,¹⁸ are found in these ionic liquids below the glass transition temperature T_g .^{10,12} To elucidate the effects of applying pressure on a supercooled liquid whose cohesive energy is influenced by Coulomb interactions, we investigate here the relaxation dynamics under high pressure of the ionic liquid 1-butyl-1-methylpyrrolidinium bis[oxalate]borate (BMP-BOB). We report on conductivity relaxation dynamics by dielectric spectroscopy measurements in the temperature range 123–300 K and pressures from 0.1 MPa to 0.5 GPa. This ionic liquid has a relatively high glass transition temperature, around 225 K at atmospheric pressure, which makes it very suitable for measurements at high pressures.

Experimental Section

The 1-butyl-1-methylpyrrolidinium bis[oxalate]borate supplied by Merck was used as received. Ambient pressure electrical measurements in the frequency range 10^{-2} – 10^7 Hz were performed with a Novocontrol Alpha Analyzer, with a parallel plate sample cell 20 mm in diameter. The temperature of the sample was controlled by a thermostatic bath with an accuracy of 0.1 K.

For the pressure-dependent dielectric measurements, we used a similar high-pressure setup and sample cell as described in ref 7. The capacitor, filled with tested material, was placed in

* Corresponding author. Telephone: +34913944435. Fax: +34913945196. E-mail: alberto.rivera@fis.ucm.es.

[†] Universidad Complutense de Madrid.

[‡] Silesian University.

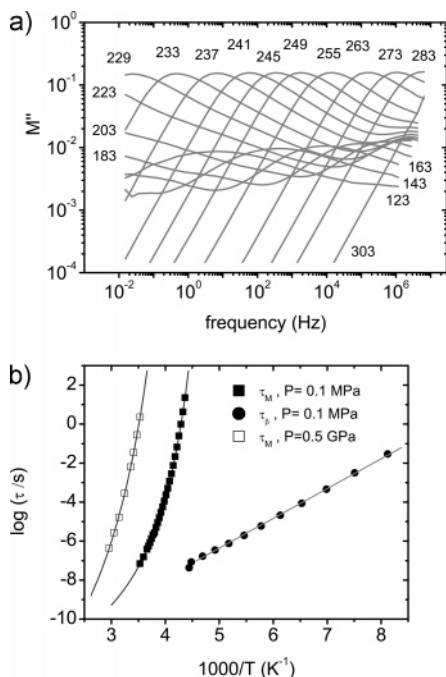


Figure 1. (a) Imaginary part of the electric modulus M'' of the ionic liquid BMP-BOB versus frequency at ambient pressure and fixed temperatures in the range 123–303 K (temperatures are shown in the figure for each curve). A main relaxation process corresponding to ionic conductivity relaxation and secondary relaxation in the glassy state appears as peaks. (b) Characteristic times of the relaxation processes of BMP-BOB in an Arrhenius representation. Main process at atmospheric pressure and 0.5 GPa, and secondary process at atmospheric pressure are shown as ■ and □, and ●, respectively. Solid lines are fits to a Vogel–Fulcher–Tammann equation in the case of the main relaxation and to an Arrhenius behavior for the secondary relaxation (see text).

the high-pressure chamber. Pressure was exerted on the chamber from a pressure generator through silicone oil. The sample capacitor was sealed and mounted inside a Teflon ring to separate the sample from the silicone. Pressure was measured by the Nova Swiss tensometric pressure meter with a resolution of 0.1 MPa. The temperature was controlled within 0.1 K by means of a liquid flow provided by a thermostatic bath.

Results and Discussion

The electric modulus M^* is a magnitude reflecting the relaxation of the macroscopic electric field at constant charge conditions and is related to the permittivity and conductivity representations $M^*(\omega) = 1/\epsilon(\omega)^*$, $M^*(\omega) = i\omega/\sigma(\omega)^*$. It shows a susceptibility behavior for ionic conductivity processes, presenting a peak or maximum in the spectral shape of M'' , and a step in the real part M' . In the ideal case of a random and independent ion motion, we would observe a frequency-independent conductivity in the whole frequency range, and the peak in the electric modulus would have a symmetric or Debye shape. Figure 1a shows the frequency dependence of $M''(\omega)$ for BMP-BOB at atmospheric pressure and different temperatures from 123 to 303 K. The electric response of this IL shows the typical behavior of an ionic conductor,^{13–16} an asymmetric peak in M'' , the maximum of which is determined by the relaxation rate of the ion diffusion process.¹⁹ The correlations among mobile ions when developing the ionic transport give rise to a frequency-independent or dc conductivity at low frequencies but to conductivity dispersion at high frequencies, and consequently to the observed asymmetry of the peak in M'' , broadening its high-frequency side.^{5,10–17,19} The characteristic

electric modulus relaxation times are thus determined from the peak positions f_M in Figure 1a as $\tau_M = 1/(2\pi f_M)$, and because the orientational and translational degrees of freedom in the supercooled regime were reported to be correlated in a similar ionic liquid, we consider these times indicative of the main structural relaxation.¹² Lowering the temperature, the relaxation peak observed in the electric modulus is shifted to lower frequencies with the same apparent activation energy as that of the dc conductivity. When τ_M increases toward 100 s, a value often used to define the glass transition temperature from dielectric measurements, another relaxation peak with a smaller strength enters our frequency window at the high-frequency end (see Figure 1a). Its characteristic time increases with decreasing temperature in a thermally activated fashion; also the relaxation peak broadens, and its amplitude or relaxation strength decreases.

Figure 1b shows the temperature dependence of the characteristic times of the relaxation processes present in BMP-BOB in an Arrhenius representation. The main relaxation, related to the ionic conductivity, shows a markedly non-Arrhenius temperature dependence, which can be well described in the whole experimental temperature range by a single Vogel–Fulcher–Tammann (VFT) law of the form (solid line in Figure 1b):

$$\tau_M = \tau_\infty \exp[E_a/k_B(T - T_0)] \quad (1)$$

At atmospheric pressure, the fit to eq 1 gives a value of $\tau_\infty = 6.6 \times 10^{-14}$ s for the infinite temperature extrapolation of the relaxation time, $E_a = 0.11$ eV (10.6 kJ/mol) for the limiting activation energy at high temperatures, and $T_0 = 191$ K. Also plotted in Figure 1b are the characteristic times of the secondary relaxation, which exhibit an Arrhenius behavior at temperatures below T_g with an activation energy of 0.3 eV (29 kJ/mol). The temperature dependence changes near T_g , and the secondary process depends steeply on $1/T$, its characteristic time being too small to enter our accessible frequency range. The pre-exponential factor (about 10^{-14} s) and the activation energy obtained from the Arrhenius fit to this relaxation (solid straight line) are typical values of the secondary relaxations observed in other conventional glass formers.^{4,5} Whether it is an intrinsic process, so-called Johari–Goldstein (JG) type,¹⁸ or not, should be elucidated by examining the pressure dependence of this relaxation.^{7,8,20,21}

The effect of applying pressure to the electric response of the IL is observed in Figure 2a, where the imaginary part of the electric modulus is plotted versus frequency at a fixed temperature, 278 K, and increasing pressures from 50 to 500 MPa. It can be observed that the main relaxation process is slowed in this pressure range from a characteristic time of the order of 10^{-6} s to much longer than 10^2 s, the longest time (lowest frequency) limit of our experimental setup. Figure 2a evidences that the secondary process is much less sensitive to pressure, because at atmospheric pressure we clearly observe this process when τ_M is below 1 s, but there is no trace of a secondary relaxation in the electric modulus spectra when τ_M is well below that value, even at the highest pressures. When further decreasing the temperature to 258 K and at the highest pressure, 0.5 GPa, the secondary process starts to appear at the high-frequency limit of our experimental window and keeps the strength of the relaxation in the order of 10^{-2} (not shown). We can conclude that pressure almost does not affect this secondary process, which indicates that it is not an intrinsic or JG relaxation, because this kind of process exhibits a significant pressure dependence similar to that of the primary or main relaxation process.^{5–8,22} In Figure 2b, the characteristic times

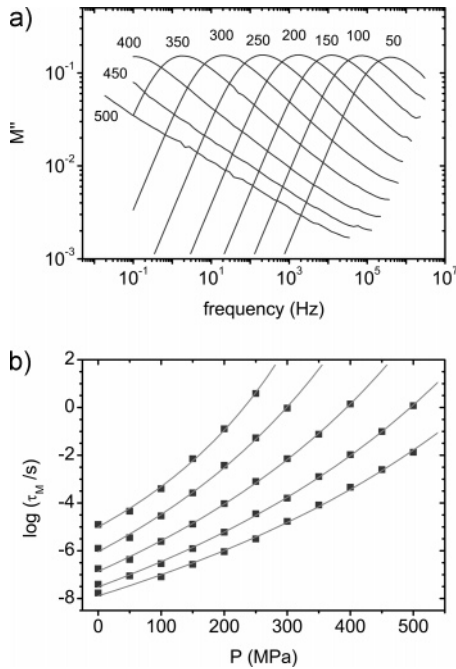


Figure 2. (a) Imaginary part of the electric modulus M'' of the ionic liquid BMP-BOB versus frequency at 278 K and fixed pressure from 50 MPa to 0.5 GPa (pressure in MPa is shown in the figure for each curve). (b) Pressure dependence of the characteristic times of the main relaxation process, the ionic conductivity relaxation, at different temperatures (258, 268, 278, 288, and 296 K, from top to bottom). Data at the two highest temperatures at atmospheric pressure are extrapolated values from the VFT fit shown in Figure 1b. Solid lines are fits to eq 4, and the fit parameters are given in Table 1.

of the main relaxation are plotted versus pressure for five different isotherms in the range from 258 to 296 K. At the two highest temperatures, 288 and 296 K, and considering the good fits of the temperature dependence of the characteristic relaxation times to the VFT law, the extrapolated value from the fit at atmospheric pressure is included in the graph to complete the data (see Figure 2b). It can be observed that the effect of increasing pressure results in an increase of the relaxation time at all temperatures.

There are several models proposed to account for the pressure and temperature dependence of the relaxation times in the dynamics of glass formers.^{5–7} A common approach is to consider the relaxation as a volume activated process,

$$\tau_M(T,P) = \tau_0(T,0) \exp(P\Delta V/RT) \quad (2)$$

with an activation volume ΔV . The times $\tau_0(T,0)$ in the above expression are the characteristic relaxation times at atmospheric pressure, and in the framework of transition state theory, the dependence of the characteristic times with pressure can be used to define the activation volume as:^{5–7}

$$\Delta V = RT \left(\frac{\partial \ln \tau}{\partial P} \right)_T \quad (3)$$

with ΔV the difference in volumes of activated and nonactivated species. However, the value of ΔV is almost never observed in experiments to be constant but to vary with both P and T , and consequently some explicit dependence on these variables must be introduced to fit the experimental data. A widely held practice is to use a dependence of the form $\Delta V = RTD_P/(P_0 - P)$, and then one obtains the equivalent of the VFT equation:^{5–7,23}

$$\tau_M(T,P) = \tau_0(T,0) \exp(D_P P / (P_0 - P)) \quad (4)$$

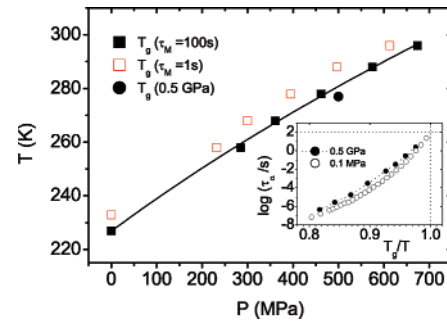


Figure 3. Pressure dependence of the glass transition temperature T_g of the ionic liquid BMP-BOB. The pressure dependence is found to be similar independently of the criterion used to define T_g , $\tau = 100$ s (■) or $\tau = 1$ s (□). T_g data at $\tau = 100$ s were obtained by extrapolating the fits to eq 4 in Figure 2b. The solid line is a fit to eq 5. The solid circle represents T_g at $\tau = 100$ s as obtained by extrapolation of the VFT fit of relaxation times at 0.5 GPa.

TABLE 1: Parameters Obtained from the Fits to Eq 4 To Describe the Pressure Dependence of the Relaxation Times at Fixed Temperature (See Solid Lines in Figure 2b)

T/K	τ_0/s	D_P	P_0/MPa
258	9.87×10^{-6}	23.6	705
268	9.13×10^{-7}	31.5	977
278	1.37×10^{-7}	32.9	1220
288	3.14×10^{-8}	32.4	1420
296	1.29×10^{-8}	29.5	1550

In fact, the latter equation can be deduced from the temperature VFT law by using the transformation $T^{-1} \propto P$, which comes from the experimental observation that lowering temperature has a similar effect on the relaxation times as does compression. Fits of the characteristic times of the main relaxation of BMP-BOB to eq 4 are shown as solid lines in Figure 2b, and the parameters obtained from the fits are listed in Table 1. It can be observed that these fits are reasonably good for all of the isotherms shown in the figure, and the pressure dependence of the relaxation times in the measured range is thus well captured by eq 4.

The good fits obtained to the pressure dependence of the relaxation times allow one to extrapolate the fits to estimate the pressure for which the relaxation time is equal to 100 s at each fixed temperature, and thus obtain the pressure dependence of the glass transition temperature $T_g(P)$. This is plotted in Figure 3. As can be observed from the solid line in Figure 3, we find that T_g of BMP-BOB can be well described by the empirical equation:^{24,25}

$$T_g = k_1(1 + k_2/k_3P)^{1/k_2} \quad (5)$$

with $k_1 = 227$, $k_2 = 2.80$, and $k_3 = 1920$. Although $T_g(P)$ values at $\tau = 100$ s were obtained by extrapolation, we would like to remark that choosing another arbitrary value of the characteristic time to define T_g results in essentially the same pressure dependence. This can be observed in Figure 3, where the pressure dependence for transition temperatures obtained by using the criterion $\tau = 1$ s is also shown for comparison. The pressure coefficient of the glass transition temperature, dT_g/dP , decreases with increasing pressure in BMP-BOB, as usually found in other glass formers,⁷ and the value in the limit of low pressures is found to be $dT_g/dP = 125$ K/GPa. This is a rather intermediate value, above the pressure coefficient of molecular glass formers, which present H-bonds like propylene glycol (37 K/GPa), glycerol (40 K/GPa), or *m*-fluoroaniline (81 K/GPa), but below that of the van der Waals materials (200–300 K/GPa).⁷

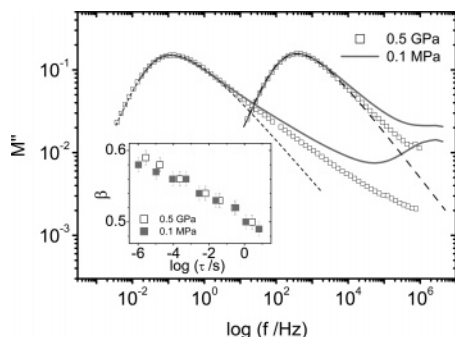


Figure 4. Electric modulus relaxation spectra (M'') of the ionic liquid BMP-BOB at ambient pressure and 231 and 245 K are plotted as solid lines. High pressure M'' data (0.5 GPa) at the temperatures that yield relaxation times similar to those of the ambient pressure data, 283 and 308 K, are included in the figure as \square . 0.5 GPa data are slightly shifted in frequency to match perfectly the atmospheric peak frequencies. Long and short dashed lines are fits to a KWW relaxation function (see text) with $\beta = 0.56$ and 0.50 , respectively. The inset shows the correlation between the stretching parameter β and the relaxation time at different temperatures and at atmospheric pressure (\blacksquare) and at 0.5 GPa (\square).

Isobaric characteristic times of the main relaxation of BMP-BOB at the highest pressure 0.5 GPa are plotted in Figure 1a as \square . The experimental data are very accurately described by using a VFT law (eq 1) with $T_0 = 202.8$ K, $\tau_0 = 5.6 \times 10^{-17}$ s, and $E_a = 0.27$ eV. An estimation of the pressure dependence of T_0 can thus be obtained, and although sometimes the pressure dependence of T_0 and T_g has been reported to be similar in the low-pressure limit, in general they exhibit different pressure dependence,^{5–7} as it is found here for BMP-BOB. It is also interesting to comment on the pressure dependence found for the isobaric fragility, $m_p \equiv d \log \tau(T_g)/d (T_g/T)_p$. In the inset to Figure 3, the temperature dependence of the relaxation times at atmospheric pressure and at 0.5 GPa is represented in a so-called Angell's fragility plot, where the slope of the data curves at $T = T_g$ directly yields the isobaric fragility. It can be observed from this plot the large value found for the isobaric fragility in this ionic liquid ($m_p = 100 \pm 10$ at 0.1 MPa), and that it decreases when increasing pressure ($m_p = 65 \pm 5$ at 0.5 GPa). Such a reduction of the fragility when increasing pressure is typically observed in glass-forming liquids, except for the case of hydrogen-bonded liquids.⁷

Finally, we address the validity of pressure–temperature superposition in ionic liquids, which is a key issue in the understanding of the glass transition from a theoretical point of view. In Figure 4, we analyze the shape of the electrical conductivity relaxation of BMP-BOB. The main panel in the figure shows the dependence of the spectral shape of M'' with temperature and pressure. The imaginary part of the electric modulus is plotted at 231 and 245 K at atmospheric pressure (solid lines), together with data at 0.5 GPa and 283 and 308 K (\square). These temperatures were chosen to have relaxation times similar to those of the isotherms measured at ambient pressure. Experimental data were very slightly shifted in frequency to match perfectly the peak frequency to that of the data at atmospheric pressure, so that the spectral shapes can be more easily compared. It can be clearly observed from Figure 4 that the pressure–temperature superposition holds in BMP-BOB for the main relaxation; that is, when the characteristic time is the same, irrespective of the specific pressure–temperature conditions, the shape of the main relaxation is also exactly the same. The only difference of the spectra at low temperatures and ambient pressure from those at higher temperatures and pressure (0.5 GPa) is the strength of the secondary relaxation, which is observed to depend very slightly on pressure, so that its

characteristic times are out of the experimental frequency window at high temperatures for any value of the pressure. To quantify the change (broadening) in the spectral shape of M'' when increasing the relaxation time τ_M by decreasing the temperature, we fit the electric modulus data to the Fourier transform of a KWW function, $f_{\text{KWW}} = \exp(-t/\tau_{\text{KWW}})^\beta$, which has been shown to describe accurately the main relaxation process in many different systems.^{16,21} These fits are shown as dashed lines in Figure 4. The exponent β is usually termed stretching parameter and accounts for the deviations observed in experimental data from a symmetric peak in M'' that would arise from a purely exponential or Debye relaxation ($\beta = 1$). Thus, the broader and more asymmetric the peak is, the lower is the value of β obtained in the fit. As it is usually found, the fits to KWW functions reproduce very well the maximum in the electric modulus and the low-frequency side of the peak, underestimating the experimental data at the highest frequencies (at least an order of magnitude higher than the peak frequency). The inset in Figure 4 shows the correlation between the relaxation time and the spectral shape of the relaxation function as given by the stretching parameter β . In the temperature range analyzed, the relaxation time τ_M increases from approximately 10^{-6} to 5 s, and the width of the relaxation peak monotonically decreases with the value of the KWW exponent decreasing from $\beta = 0.59 \pm 0.01$ to $\beta = 0.49 \pm 0.01$. As temperature decreases the relaxation time increases, and the relaxation function slows down in a way that temperature–pressure superposition holds. Data in the inset of Figure 4 are presented for two different values of applied pressure ($P = 0.1$ MPa and $P = 0.5$ GPa), and it can be observed that, within experimental error, the value of β is the same for a given relaxation time, independently of the pressure–temperature conditions. This finding strengthens the importance of the temperature–pressure superposition as a model-independent experimental fact that should be incorporated in any theory or model of the glass transition. Most of the current theories or models consider separately the pressure–temperature dependence of the structural relaxation time and the slowing (stretching) of the relaxation, and thus are not able to account for this experimental finding. In fact, to our knowledge, the only exception is the Coupling Model approach.⁸

Conclusions

In summary, we have investigated the effects of applying high pressure on the electrical conductivity relaxation in a liquid ionic conductor, the ionic liquid 1-butyl-1-methylpyrrolidinium bis-[oxalate]borate. We find that the dynamic response under pressure in this ionic liquid is similar to that of nonionic glass formers. We analyzed the pressure dependence of the glass transition temperature and found that previously proposed models account for the experimental results. A secondary relaxation process, weakly depending on pressure, is observed, but the main relaxation process shows temperature–pressure superposition. Thus, the spectral shape of the main relaxation broadens with increasing pressure or decreasing temperature, but is found to be the same when the relaxation time is the same, whatever the combination of pressure and temperature values.

Acknowledgment. We thank K. L. Ngai for fruitful discussions. A.R.-C. is thankful for financial support from the Ramon y Cajal program. Work at Universidad Complutense is sponsored by Spanish MEC (MAT 2004-3070-C05-02).

References and Notes

- (1) Welton, T. *Chem. Rev.* **1999**, *99*, 2071.
- (2) Wasserscheid, P.; Keim, W. *Angew. Chem., Int. Ed.* **2000**, *39*, 3772.

- (3) *Ionic Liquids in Synthesis*; Wasserscheid, P., Welton, T., Eds.; Wiley-VCH: Weinheim, Germany, 2003.
- (4) Schneider, U.; Lunkenheimer, P.; Brand, R.; Loidl, A. *Phys. Rev. E* **1999**, *59*, 6924.
- (5) Kremer, F.; Schönhals, A. *Broadband Dielectric Spectroscopy*; Springer: New York, 2002.
- (6) Floudas, G. *Prog. Polym. Sci.* **2004**, *29*, 1143.
- (7) Roland, C. M.; Hensel-Bielowka, S.; Paluch, M.; Casalini, R. *Rep. Prog. Phys.* **2005**, *68*, 1405.
- (8) Ngai, K. L.; Casalini, R.; Capaccioli, S.; Paluch, M.; Roland, C. *M. J. Phys. Chem. B* **2005**, *109*, 17356.
- (9) Xu, W.; Cooper, E. I.; Angell, C. A. *J. Phys. Chem. B* **2003**, *107*, 6170.
- (10) Rivera, A.; Roessler, E. A. *Phys. Rev. B* **2006**, *73*, 212201.
- (11) Ito, N.; Huang, W.; Richert, R. *J. Phys. Chem. B* **2006**, *110*, 4371.
- (12) Rivera, A.; Brodin, A.; Pugachev, A.; Roessler, E. A. *J. Chem. Phys.* **2007**, *126*, 114503.
- (13) Angell, C. A. *Chem. Rev.* **1990**, *90*, 523.
- (14) Funke, K. *Prog. Solid State Chem.* **1993**, *22*, 111.
- (15) Ngai, K. L.; León, C. *Solid State Ionics* **1999**, *125*, 81.
- (16) Ngai, K. L.; León, C. *Phys. Rev. B* **2002**, *66*, 064308.
- (17) Pimenov, A.; Lunkenheimer, P.; Rall, H.; Kohlhaas, R.; Loidl, A. *Phys. Rev. E* **1996**, *54*, 676.
- (18) Johari, G. P.; Goldstein, M. *J. Chem. Phys.* **1970**, *53*, 2372.
- (19) Hodge, I. M.; Ngai, K. L.; Moynihan, C. T. *J. Non-Cryst. Solids* **2005**, *351*, 104.
- (20) León, C.; Ngai, K. L.; Roland, C. M. *J. Chem. Phys.* **1999**, *110*, 11585.
- (21) Ngai, K. L.; Lunkenheimer, P.; León, C.; Schneider, U.; Brand, R.; Loidl, A. *J. Chem. Phys.* **2001**, *115*, 1405.
- (22) Ngai, K. L.; Paluch, M. *J. Chem. Phys.* **2004**, *120*, 857.
- (23) Paluch, M.; Patkowski, A.; Fischer, E. W. *Phys. Rev. Lett.* **2000**, *85*, 2140.
- (24) Andersson, S. P.; Andersson, O. *Macromolecules* **1998**, *35*, 2999.
- (25) Avramov, I. *J. Non-Cryst. Solids* **2005**, *351*, 3163.